analytical chemistry

pubs.acs.org/ac Article

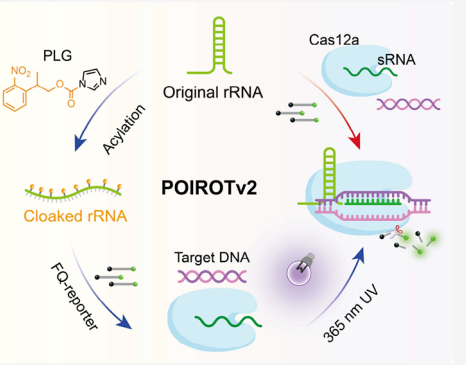
Plug-and-Play Photo-Initiated CRISPR–Cas12a One-Pot Nucleic Acid Detection via Universal Repeat RNA Acylation Strategy

Jinlian Du,[#] Xingxiang Pu,[#] Tongyan Yuan, Fang Peng, Jingjing Hu, Han Li, Bojie Chen, Jiaming Luo, Sheng Li, Yuling Teng, Xinyue Zhu, Weiming Chen, Qingqing Xie, Ling Jiang,* Erhu Xiong,* and Ronghua Yang

Cite This: https://doi.org/10.1021/acs.analchem.5c05769 Read Online

ACCESS | Metrics & More | Article Recommendations | Supporting Information

ABSTRACT: Precise spatiotemporal control of CRISPR activity is central to both accurate gene editing and sensitive molecular diagnostics. However, current regulatory strategies are often sequence-specific, labor-intensive, and difficult to generalize. Here, we report a minimalist plug-and-play tactic: acylation of the repeat region (rRNA) of a split crRNA with photolabile groups. Because the modification is introduced post-synthesis and is independent of the spacer region (sRNA), every rRNA, regardless of its target sequence, can be activated by light irradiation alone, entirely eliminating the need for redesign or reoptimization. Integrating the photo-initiated CRISPR–Cas12a system with recombinase polymerase amplification into a one-pot format yields an upgraded platform, named POIROTv2 (PhotO-Initiated CRISPR–Cas12a system for Robust One-pot Testing, version 2). POIROTv2 achieves a 100-fold sensitivity gain over conventional always-on Cas12a-based one-pot assays and matches the analytical performance of a two-step assay while remaining a more streamlined and potentially faster detection process and avoiding the risk of aerosol contamination. In clinical validation with HCMV- and EBV-suspected samples, POIROTv2 delivered diagnostic accuracy statistically indistinguishable from that of gold-standard qPCR, highlighting its potential for robust and sensitive molecular diagnostics. Overall, the strategy opens up exciting possibilities for applications in infectious virus diagnostics and has broad prospects in the field of spatiotemporally controllable gene editing.



INTRODUCTION

In recent years, the prevalence of viruses, such as SARS-CoV-2, influenza variants, and monkeypox, has increased global attention on the surveillance and control of infectious viruses.[1] Therefore, accurate and effective nucleic acid testing has become particularly important. The ideal nucleic acid testing technology should possess high sensitivity and specificity while also being rapid, easy to operate, and cost-effective.[2,3] Currently, gene sequencing[4] and polymerase chain reaction (PCR)[5] are widely adopted nucleic acid testing methods and are regarded as the "gold standard" in this field. Although they deliver excellent analytical performance, both methods are time-consuming and require sequencers or thermocyclers, which severely limits their convenience and accessibility for rapid and broad applications.[6] Isothermal nucleic acid amplification reactions, such as loop-mediated isothermal amplification (LAMP)[7] and recombinase polymerase amplification (RPA),[8] represent a class of innovative and emerging nucleic acid amplification technologies that have garnered significant attention over the past two decades. These methods can be performed at a constant temperature, thereby eliminating the need for the time-consuming thermal cycling process in traditional PCR. By bypassing the repetitive denaturation and annealing steps required for PCR, isothermal amplification methods also eliminate the dependence on sophisticated temperature control equipment, making them more suitable for point-of-care testing and field-deployable applications.[9,10] However, despite their advantages, these methods often suffer from nonspecific amplification, which compromises the accuracy of detection results.[11]

Over the past decade, the CRISPR (clustered regularly interspaced short palindromic repeats)/Cas (CRISPR-associated) system has gained rapid traction and development, thanks to its remarkable capabilities for precise molecular recognition, specific targeting, and efficient signal amplification.[12−19] These intrinsic features have endowed the CRISPR system with unique advantages in both gene editing and molecular diagnostics, positioning it as a transformative tool in the fields of molecular biology and biomedical research.[19,20]

Received: September 16, 2025
Revised: December 22, 2025
Accepted: January 6, 2026

Downloaded via SHANGHAI NORMAL UNIV on January 17, 2026 at 02:42:47 (UTC).
See https://pubs.acs.org/sharingguidelines for options on how to legitimately share published articles.

ACS Publications © XXXX American Chemical Society

The fundamental principle of the CRISPR system is to design appropriate CRISPR RNA (crRNA), which consists of a conserved repeat RNA (rRNA) and a variable spacer RNA (sRNA).[21−28] Subsequently, under the guidance of crRNA in either full-length or split form, the Cas protein/crRNA complex binds to target DNA strands to trigger its dual enzymatic activities: specific *cis*-cleavage on the target DNA strand and nonspecific *trans*-cleavage of nearby single-stranded DNA (ssDNA)/ssRNA.[29−32] Taking the CRISPR−Cas12a system as an example, once activated by target DNA, it exhibits nonspecific cleavage activity toward ssDNA reporter probes, generating amplified detection signals that achieve picomolar-level sensitivity.[8,33] However, it still falls short of the clinical demand for highly sensitive detection. To address this limitation, researchers commonly integrate the CRISPR system with isothermal amplification techniques to further enhance the detection sensitivity. Common methods include DETECTR,[32] SHERLOCK,[34] and HOLMES,[35] etc. Although significant strides have been made in improving detection sensitivity, these conventional approaches that separately conduct nucleic acid amplification and CRISPR detection present several critical challenges. Specifically, they inherently involve cumbersome operational procedures that are time-consuming and require highly skilled personnel. Moreover, this multistep process also heightens the risk of nucleic acid aerosol contamination, potentially generating false-positive results and undermining overall assay reliability.[36−38]

Recent studies have successfully demonstrated the feasibility of combining isothermal amplification with CRISPR detection into a one-step reaction.[39−41] However, these approaches face a significant challenge due to the inherent incompatibility between the two systems. The fundamental issue arises when the CRISPR system becomes activated; its robust cleavage activity specifically cuts the amplification templates and indiscriminately degrades the amplification primers, thereby compromising amplification efficiency and ultimately diminishing detection sensitivity. To address this issue, two primary strategies have been employed: physical spatial separation[42−44] and CRISPR activity regulation.[37,45−51] While physical isolation methods (e.g., compartmentalization or barrier-based partitioning) can be effective, they often require high operational precision and additional handling steps, such as centrifugation, which increases both complexity and the risk of cross contamination. Alternatively, regulating CRISPR activity can be achieved through protein engineering (e.g., generation of Cas protein mutants) or crRNA modifications. Nevertheless, engineering Cas enzymes via site-directed mutagenesis frequently faces a trade-off between catalytic activity and controllability.[37,47] Light has been widely employed as an ideal tool for the remote control of CRISPR activity with high spatiotemporal precision, finding extensive applications in gene editing regulation and molecular diagnostics.[46−53] Light-based crRNA regulation strategies, such as antisense blockers[48,49] and photocaged nucleotides,[50,51] provide more flexible control, but each new target necessitates the redesign, synthesis, and experimental validation of tailored oligonucleotides. These iterative optimization processes are not only laborious and time-consuming but also restrict the generalizability and scalability of the method.[54] Our group recently developed a simple acylation strategy to modify photolabile agents (PLGs) at the 2′-OH group of crRNAs, effectively deactivating the CRISPR system. Upon light irradiation, the PLGs are released, restoring the CRISPR system's activity.[55] Based on this principle, we further established a one-pot nucleic acid detection platform, termed POIROT (PhotO-Initiated CRISPR−Cas12a system for Robust One-pot Testing). Although the acylation reaction is independent of RNA sequence changes, each new detection target requires reacylation of the corresponding crRNA, inevitably introducing additional complexity and uncertainty to the detection process.

Herein, we present an upgraded version of the POIROT system, termed POIROT version 2 (POIROTv2). In this version, we specifically acylate the repeat region (rRNA) of the split crRNA, rather than the full-length crRNA. The acylated rRNA cannot form a stable complex with the Cas12a protein, thereby deactivating the CRISPR system. Since the acylation process does not involve the spacer region (sRNA), alterations in the target sequence do not impact the overall design, enabling the strategy to function as a truly "plug-and-play" universal regulation manner for CRISPR activity regardless of target variations. Compared with traditional one-pot methods, the POIROTv2 assay is straightforward and highly adaptable, eliminating the need for protein engineering and tedious trial-and-error screening. More importantly, the updated one-pot biosensing platform demonstrates superior detection performance compared with traditional one-pot methods. It also achieves analytical performance comparable to that of the two-step methods while simplifying the operational workflow and reducing the risk of aerosol contamination. When applied to clinical samples, POIROTv2 shows high concordance with the gold-standard qPCR method. Overall, this method offers broad application potential in nucleic acid detection, disease diagnosis, and biomedical research. Moreover, it can be readily adapted to other CRISPR−Cas12 systems such as ErCas12a and AsCas12a, further expanding its utility and impact.

EXPERIMENTAL SECTION

Polyacrylamide Gel Electrophoresis (PAGE) Analysis of the Cloaking and Photo-Induced Uncloaking of rRNA

The rRNA was acylated with different acylation durations. Then, the cloaked rRNA (5 μL) was mixed with 6× loading dye (1 μL) and loaded into a 12% PAGE, run at 100 V for 55 min. After that, the gel was stained with GelRed for 20 min and imaged using a ChemiDoc Imaging System (Bio-Rad, USA). Five μL of effectively cloaked rRNA (1 μM) was irradiated with 365 nm UV light for 0, 10, 20, 30, or 60 s, followed by the addition of 1 μL of 6× loading dye. Each mixture was loaded into a 12% PAGE and run at 100 V for 55 min. After that, the gel was stained with GelRed and imaged using a ChemiDoc Imaging System (Bio-Rad, USA).

Conventional CRISPR−Cas12a Fluorescence Assay for Synthetic Target dsDNA

Twenty μL of reaction solution, including LbCas12a (50 nM), rRNA (100 nM), sRNA (100 nM), FQ-reporter (250 nM), and various concentrations of dsDNA target (DEPC-treated water used as a control) in 1× LbCas12a reaction buffer, was incubated at 37 °C for 90 min on a Thermal Cycler Dice Real-Time System III (TaKaRa), and the fluorescence signals were acquired every minute.

Photo-Initiated CRISPR−Cas12a Fluorescence Assay for Synthetic dsDNA Target

Twenty μL of reaction solution, including LbCas12a (50 nM), effectively cloaked rRNA (100 nM), sRNA (100 nM), FQ-reporter (250 nM), and various concentrations of dsDNA target (DEPC-treated water used as a control) in 1× LbCas12a reaction buffer, was irradiated with a UV lamp (λ = 365 nm, 123 mW cm^{-2}). Next, the solution was incubated at 37 °C for 90 min on a Thermal Cycler Dice Real-Time System III (TaKaRa), and the fluorescence signals were acquired every minute.

https://doi.org/10.1021/acs.analchem.5c05769
Anal. Chem. XXXX, XXX, XXX−XXX

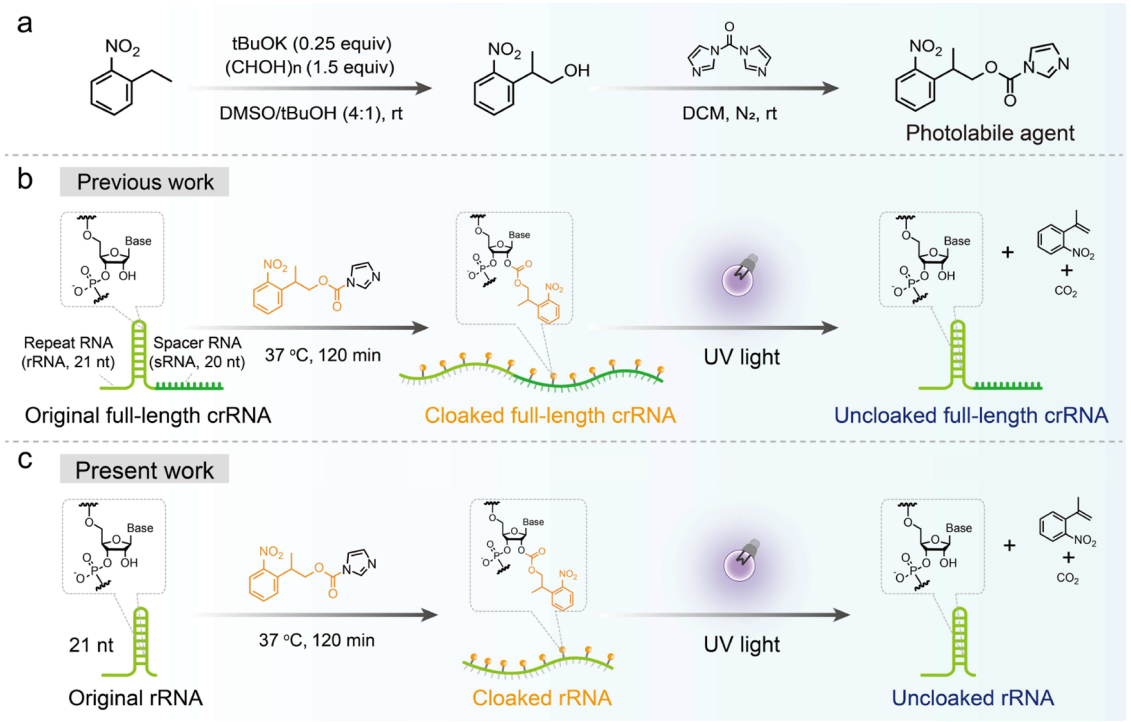


Figure 1. PLG-mediated rRNA cloaking and UV light-induced uncloaking. (a) Synthetic route of the PLGs. (b, c) Mechanism of the acylation strategy for crRNA/rRNA. PLGs installed on the 2′-OH groups of crRNA (b)/rRNA (c) strand disrupt its stem-loop structure and abolish its function; 365 nm UV light irradiation (123 mW cm^{-2}) removes the PLGs and instantly restores crRNA/rRNA structure and function.

POIROTv2 Assay for HCMV and EBV Plasmid DNA

The CRISPR−Cas12a detection system includes 50 nM LbCas12a, 100 nM effectively cloaked rRNA, 100 nM sRNA, 1× LbCas12a reaction buffer, 250 nM FQ-reporter, and DEPC-treated water. The RPA reaction system contains 2 μL of HCMV or EBV plasmid DNA with various concentrations, forward and reverse primers (0.64 μM each), 5 μL of suspended RPA mixture, 1 μL of Buffer B, and DEPC-treated water. The entire system was incubated at 37 °C for 20 min in a Thermal Cycler Dice Real-Time System III (TaKaRa) to complete the RPA step, then the mixture was exposed to 365 nm UV light (123 mW cm^{-2}) for 1 min to trigger uncloaking, followed by real-time monitoring at 37 °C for another 70 min.

Nucleic Acid Extraction of HCMV- and EBV-Suspected Clinical Samples

The genomic DNA of clinical HCMV- and EBV-suspected samples used in this study was extracted from clinical bronchoalveolar lavage fluid samples by heating at 95 °C for 5 min. The obtained DNA products were stored at −80 °C for further use.

qPCR Assay for HCMV- and EBV-Suspected Clinical Samples

A 20 μL reaction solution was prepared, containing qPCR Premix Ex Taq™, forward and reverse primers (200 nM each), 200 nM TaqMan probe, and 2 μL of HCMV- or EBV-suspected clinical sample added to the solution. The reaction solution was monitored by the Thermal Cycler Dice Real-Time System III (TaKaRa). The qPCR thermal cycling program is set as follows: pre-denaturation at 95 °C for 5 min, followed by 42 cycles of amplification at 94 °C for 15 s and 57 °C (HCMV)/60 °C (EBV) for 30 s. According to the manufacturer's protocol of the kit, the criteria are defined as C_t value ≤40 is positive, C_t value >40 is negative.

POIROTv2 Assay for HCMV- and EBV-Suspected Clinical Samples

The CRISPR−Cas12a detection system includes 50 nM LbCas12a, 100 nM effectively cloaked rRNA, 100 nM sRNA, 1× LbCas12a reaction buffer, 250 nM FQ-reporter, and DEPC-treated water. The RPA reaction system contains 2 μL of HCMV- and EBV-suspected clinical sample DNA, forward and reverse primers (0.64 μM each), 5 μL of suspended RPA mixture, 1 μL of Buffer B, and DEPC-treated water. The entire system was incubated at 37 °C for 20 min in a Thermal Cycler Dice Real-Time System III (TaKaRa) to complete the RPA step, then the mixture was exposed to 365 nm UV light (123 mW cm^{-2}) for 1 min to trigger uncloaking, followed by real-time monitoring at 37 °C for another 70 min.

RESULTS AND DISCUSSION

PLG-Mediated rRNA Cloaking and UV Light-Induced Uncloaking

The crRNA consists of two functional regions: the rRNA (repeat region) and sRNA (spacer region). The rRNA, characterized by its conserved sequence and stable stem-loop structure, serves as a universal scaffold across multiple CRISPR systems. It provides a high-affinity binding interface that facilitates efficient recognition and complex formation with various Cas proteins (Cas9, Cas12, Cas13, etc.), thereby enabling the assembly of functional ribonucleoprotein (RNP) complexes. By installing photo-responsive PLGs on the 2'−OH groups of the rRNA strand, we aim to develop a "plug-and-play" universal strategy to regulate CRISPR-Cas12a (*Lachnospiraceae bacterium* ND2006, LbCas12a) activity. To this end, we first synthesized PLG and characterized it using ^{1}H NMR spectroscopy (Figures 1a and S1, S2). In our previous work, we successfully demonstrated that PLGs can be effectively modified on the full-length crRNA, which comprises 41 nucleotides (Figure 1b). However, when it comes to rRNA, the situation is quite different. rRNA is significantly shorter, containing only 21 nucleotides (Figure 1c and Table S1). Given its markedly abbreviated length, a pivotal question arises: can PLG be effectively modified on such a concise RNA scaffold?

https://doi.org/10.1021/acs.analchem.5c05769
Anal. Chem. XXXX, XXX, XXX−XXX

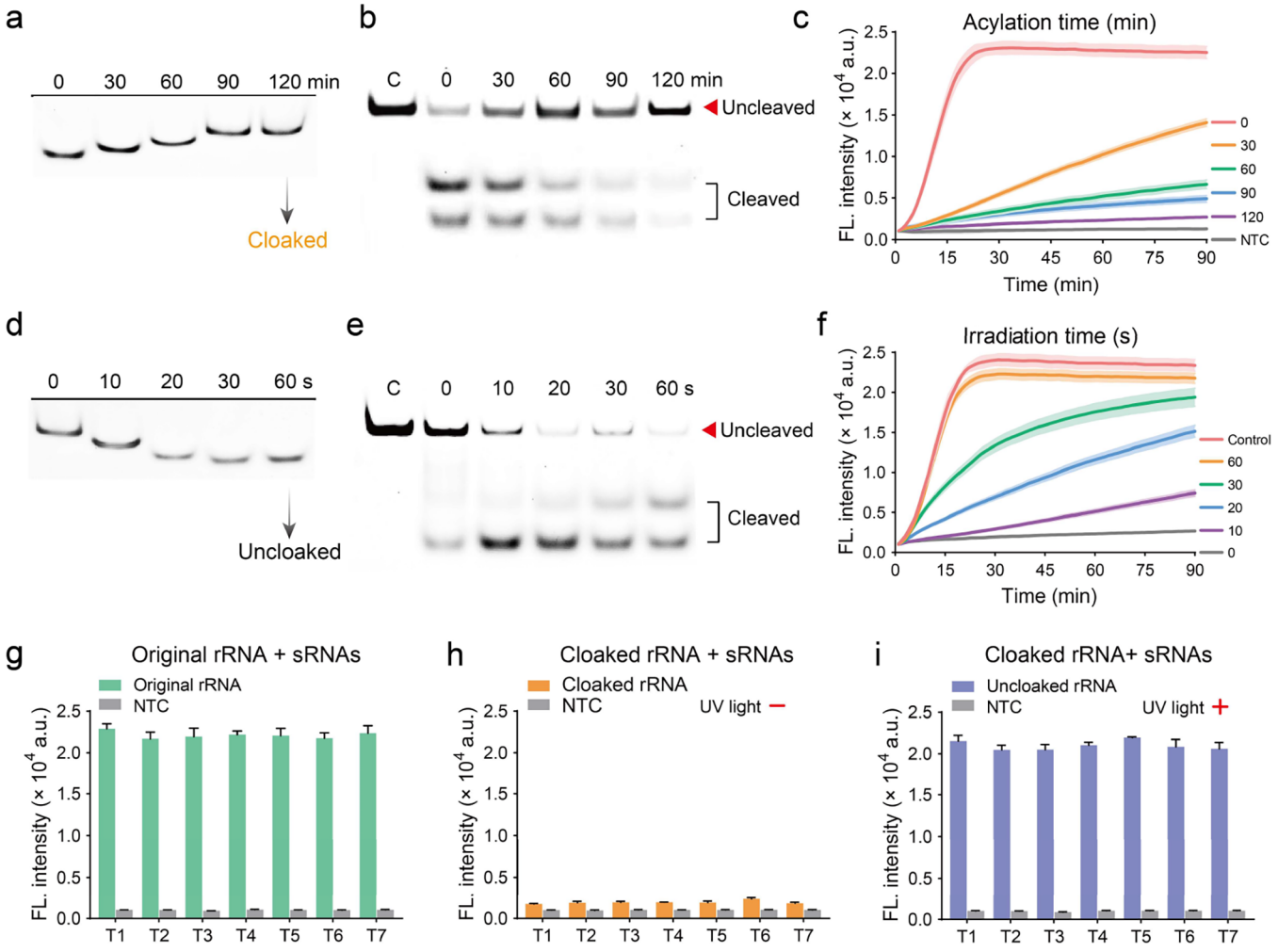


Figure 2. Effect of cloaking and photo-induced uncloaking of rRNA on the CRISPR−Cas12a system. (a) PAGE analysis of rRNA cloaking with different acylation durations (0, 30, 60, 90, and 120 min). The rRNA was treated with PLGs at 37 °C with different durations and analyzed by 12% PAGE. (b, c) PAGE analysis (b) and fluorescence kinetic analysis (c) of the *cis*-cleavage activity of the CRISPR−Cas12a system using rRNA with different acylation durations. (d) PAGE analysis of photo-induced uncloaking of rRNA. The PLG-cloaked rRNA was exposed to 365 nm UV light irradiation with various durations (0, 10, 20, 30, and 60 s), followed by 12% PAGE analysis. (e, f) PAGE analysis (e) and fluorescence kinetic analysis (f) of the *trans*-cleavage activity of the CRISPR−Cas12a system after exposing PLG-cloaked rRNA to 365 nm UV for increasing irradiation time. (g−i) Fluorescence analysis of original rRNA (g), cloaked rRNA without UV light irradiation (h), and cloaked rRNA with UV light irradiation (i) in the presence of various targets (T1−T7) and their corresponding sRNAs. The fluorescence intensities at t = 40 min are shown. C, control; NTC, no-target control; and T, target. Fluorescence analyses were conducted in triplicate, and data were represented as mean ± standard deviation.

To address this, we systematically examined both PLG-mediated rRNA cloaking and its subsequent UV light-induced uncloaking (Figure 1c). As shown in Figure 2a, the electrophoretic migration of rRNA gradually decreases with an extended acylation time, reflecting the progressive attachment of PLGs to the rRNA strand. The migration shift reaches a plateau after 120 min, suggesting that complete cloaking of the rRNA is achieved within this period. We further evaluated the influence of acylation time on CRISPR−Cas12a activity. The *cis*-cleavage activity was first examined via PAGE (Figure 2b). When rRNA was not acylated, two distinct cleavage bands were clearly visible. With increasing acylation time, these cleavage products gradually diminished. After 120 min of acylation, the cleaved bands became very faint, indicating the highly efficient suppression of the CRISPR−Cas12a system's *cis*-activity. This suppression is likely attributable to conformational changes in the acylated rRNA, which impair its binding affinity for the Cas12a protein.[56,57] For evaluating the *trans*-cleavage activity, we performed the fluorescence kinetic analysis (Figure 2c). The results indicated that the reaction rate of the fluorescent signal gradually declined as acylation time increased. Although residual fluorescence could still be detected after 120 min of acylation, its intensity was nearly indistinguishable from that of the negative control, particularly within the initial 30 min. This suggests that the residual activity is unlikely to interfere with the nucleic acid amplification. We next evaluated the stability of acylated rRNA at room temperature (~25 °C) versus −20 °C. The results indicated that low temperature is critical for the long-term storage stability of acylated RNA, as it significantly suppresses its degradation (Figures S3 and S4). Furthermore, based on our previous finding[8] that approximately 12 PLGs are sufficient to inactivate the CRISPR−Cas12a system on a full-length crRNA (41 nt), we sought to determine the number of PLG modifications required to achieve complete inactivation on the shorter rRNA strand (21 nt). Mass spectrometry was

https://doi.org/10.1021/acs.analchem.5c05769
Anal. Chem. XXXX, XXX, XXX−XXX

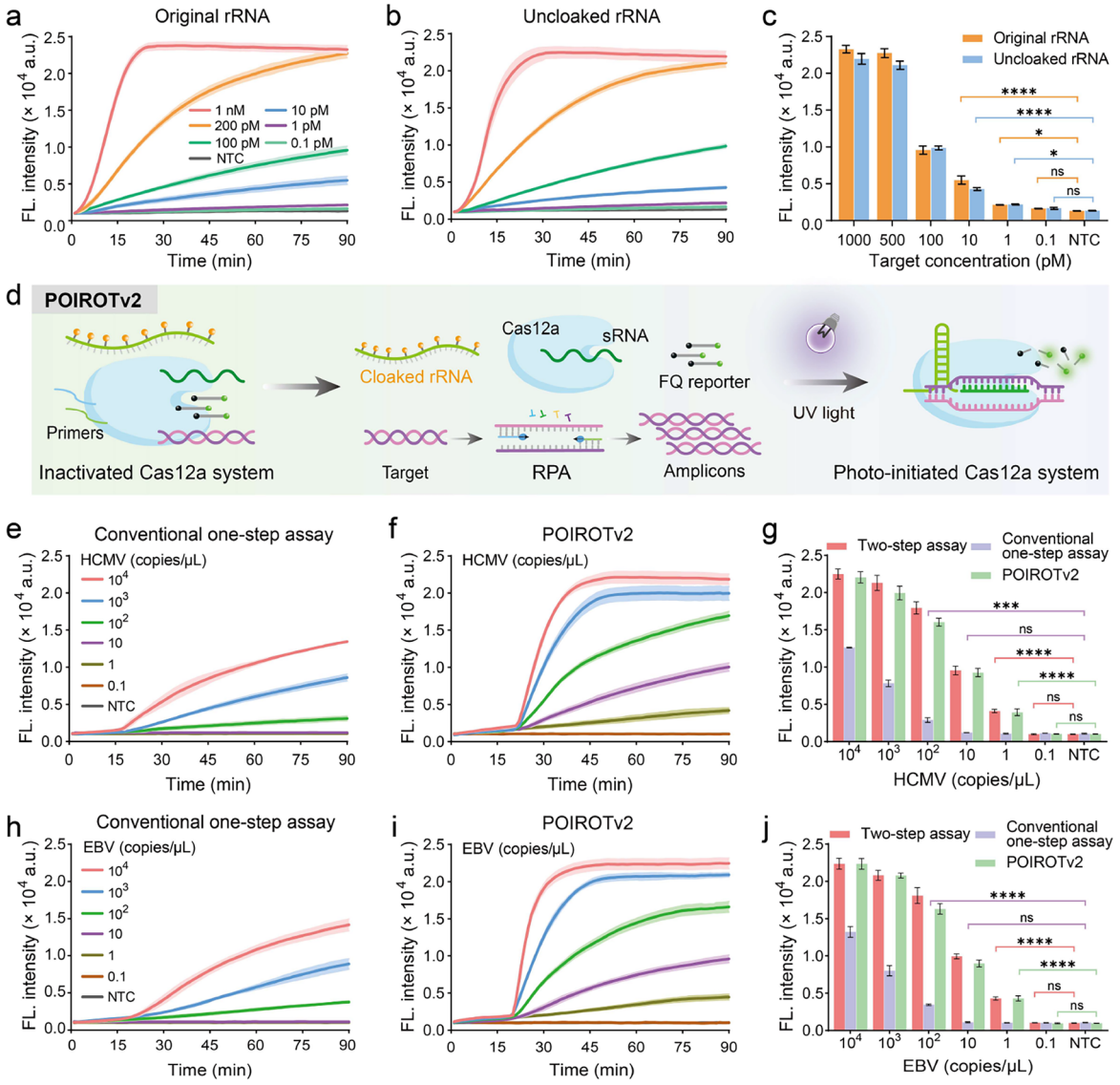


Figure 3. Establishment of POIROTv2 for nucleic acid assay. (a, b) Sensitivity analysis of the CRISPR-Cas12a system using original rRNA (a) and photo-initiated uncloaked rRNA (b) with different target concentrations. (c) Fluorescence intensities at t = 90 min of the curves in (a, b). (d) Schematic illustration of the POIROTv2 platform, coupling RPA with the photo-initiated CRISPR−Cas12a system. (e, f) Sensitivity analysis of conventional one-step assay (e) and POIROTv2 assay (f) for the detection of HCMV plasmid DNA. (g) Fluorescence intensities at t = 80 min of the curves in (e, f). (h, i) Sensitivity analysis of conventional one-step assay (h) and POIROTv2 assay (i) for the detection of EBV plasmid DNA. (j) Fluorescence intensities at t = 80 min of the curves in (h, i). NTC, no-template control. Fluorescence analyses were conducted in triplicate, and data were represented as mean ± standard deviation. Two-tailed Student's t-test; ****p < 0.0001; ***p < 0.001; **p < 0.01; *p < 0.05; ns, not significant.

employed to answer this question. Since each acylation event at the 2′-OH group of ribose with a PLG molecule increases the molecular weight by 208 Da, we analyzed the fully acylated rRNA and observed a mass shift consistent with the incorporation of approximately 4−5 PLGs (Figures S5 and S6), indicating that these PLG modifications are sufficient to fully inactivate the CRISPR−Cas12a system.

Having successfully cloaked the rRNA, we next investigated whether UV light exposure could remove the PLGs and restore its functionality. To test this, the fully cloaked rRNA was irradiated with different intensities of 365 nm UV light, including 68, 123, and 233 mW cm^{-2}. The results indicated that lower light intensity is suboptimal due to its slower activation efficiency, while excessively high light intensity may conversely inhibit CRISPR system activity, leading to a reduction in the activation rate (Figure S7). Given that the light intensity of 123 mW cm^{-2} achieves the fastest fluorescence signal output efficiency and the strongest signal intensity, it was identified as the relatively optimal experimental condition. Under this condition, as shown in Figure 2d, the electrophoretic migration of the rRNA increased with prolonged UV light exposure, indicating the gradual release of the PLGs. After 60 s of irradiation, the rRNA returned to a fully uncloaked state. Both PAGE analysis and fluorescence kinetics confirmed that 60 s of UV light irradiation effectively restored the *cis*- and *trans*-activity of the CRISPR−Cas12a system (Figure 2e,f). Additionally, the UV light-induced uncloaking of rRNA is also suitable for other Cas12a orthologues, such as ErCas12a and AsCas12a (Figure S8). Together, these results demonstrate that the activity of

https://doi.org/10.1021/acs.analchem.5c05769
Anal. Chem. XXXX, XXX, XXX−XXX

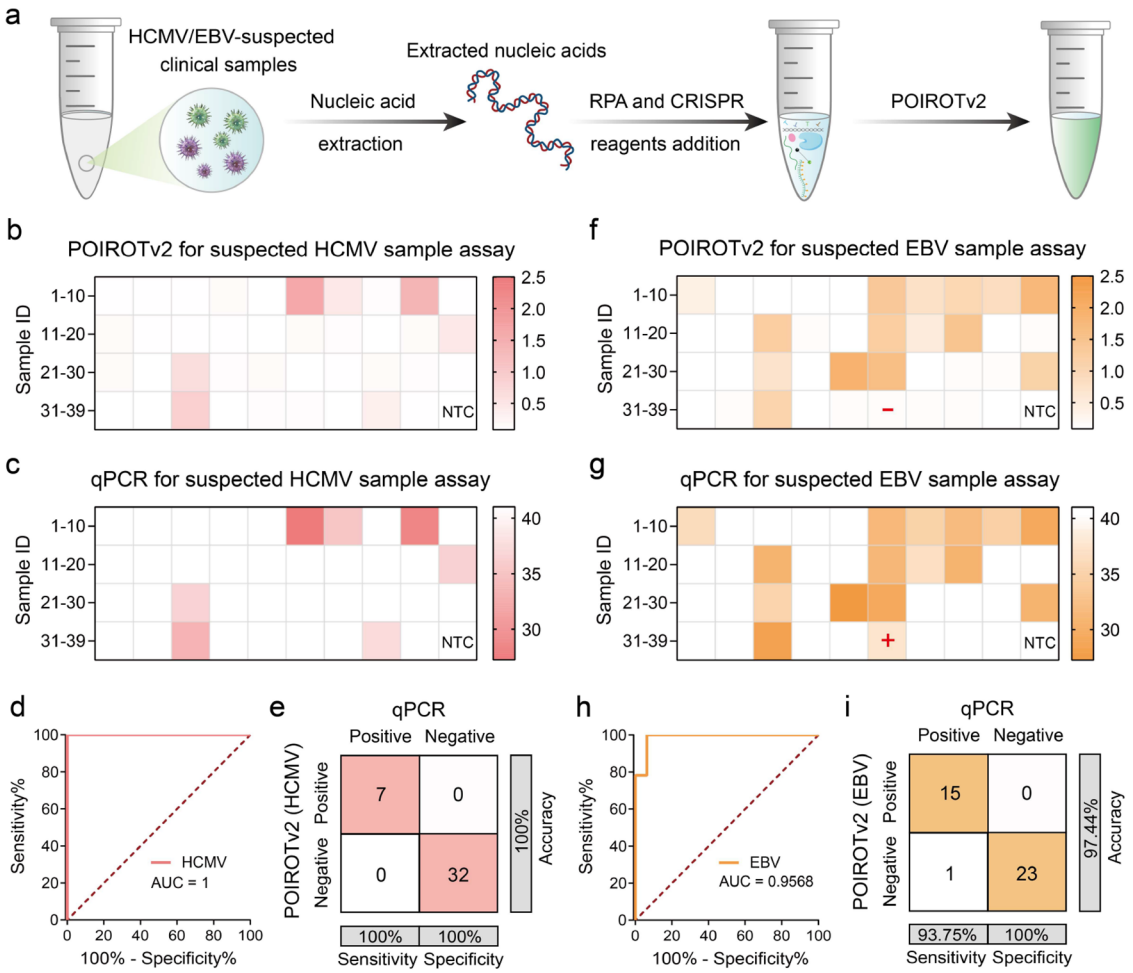


Figure 4. Clinical application of POIROTv2 for detecting HCMV- and EBV-suspected samples. (a) Schematic illustration of POIROTv2 for the HCMV and EBV sample assay in bronchoalveolar lavage fluid samples. (b) Clinical HCMV-suspected sample assay by POIROTv2. (c) Clinical HCMV-suspected sample assay by qPCR. (d) ROC curve of POIROTv2 for the detection of HCMV-suspected samples. (e) Evaluation of the clinical sensitivity, specificity, and accuracy of POIROTv2 by comparison to qPCR using a confusion matrix for the detection of HCMV-suspected samples. (f) Clinical EBV-suspected sample assay by POIROTv2. (g) Clinical EBV-suspected sample assay by qPCR. (h) ROC curve of POIROTv2 for the detection of EBV-suspected samples. The one EBV-suspected sample that failed detection is labeled with "−" in (f) and "+" in (g), respectively. (i) Evaluation of the clinical sensitivity, specificity, and accuracy of POIROTv2 by comparison to qPCR using a confusion matrix for the detection of EBV-suspected samples.

CRISPR−Cas12a system can be reversibly suppressed by acylating the 2′-OH groups of rRNA with PLGs, and subsequently restored through light-triggered deprotection.

Additionally, as a control, the original rRNA remained unaffected by UV light irradiation (Figure S9). To further assess the universality of our light-activated CRISPR−Cas12a system, we randomly selected seven new nucleic acid targets (T1−T7), each paired with its corresponding sRNA (Figure S10). The results showed that in the presence of original rRNA, all targets robustly activated the CRISPR system (Figure 2g). In contrast, the acylated rRNA completely abolished this activity (Figure 2h). Upon UV light irradiation, the fluorescence signal was robustly restored across all targets (Figure 2i). These results confirm that our rRNA-based photoactivatable CRISPR strategy operates in a truly "plug-and-play" manner: regardless of the target sequence, no redesign, resynthesis, or reoptimization is required, as every reaction employs the same acylated rRNA strand, ensuring broad versatility and ease of use.

Viral Plasmid DNA Detection by POIROTv2

Having obtained a highly effective photo-responsive CRISPR−Cas12a system, we next established the POIROTv2 platform for the detection of viral plasmid DNA. In this section, human cytomegalovirus (HCMV) and Epstein−Barr virus (EBV)—members of the β- and γ-herpesvirus subfamilies, respectively, and both known for high transmissibility—were selected as model targets. Their rapid and accurate detection is critical for early stage infection screening, outbreak containment, and therapeutic guidance. Prior to detecting EBV and HCMV, we compared the detection sensitivity of UV-deprotected (uncloaked) rRNA and the original unmodified rRNA. Fluorescence kinetics revealed that the detection sensitivity of the photo-restored rRNA was comparable to that of the original rRNA (Figure 3a−c), indicating that acylation and subsequent photoactivation of rRNA do not impair the analytical performance of the CRISPR−Cas12a system. Building on these findings, we established the POIROTv2 platform by integrating the RPA reaction with CRISPR−Cas12a detection in a one-pot system (Figure 3d) and further validated its feasibility through a component-removal experi-

https://doi.org/10.1021/acs.analchem.5c05769
Anal. Chem. XXXX, XXX, XXX−XXX

ment (Figure S11). No fluorescent signal was observed in the absence of UV light irradiation, even when all other essential components were present. In contrast, strong fluorescence was detected upon UV light irradiation, confirming the excellent light-dependent feasibility of POIROTv2. Furthermore, we compared the analytical capability of POIROTv2 with that of the two-step assay and the conventional one-step method. As shown in Figure 3e−g, POIROTv2 achieved a detection sensitivity as low as 1 copy/μL for HCMV plasmid DNA, matching the performance of the two-step assay (Figure S12) and surpassing the traditional one-step method, which only reached 100 copies/μL, by 2 orders of magnitude. Consistent results were obtained in the detection of EBV plasmid DNA across all three platforms (Figures 3h−j and S13), indicating superior analytical performance compared to that of other CRISPR one-pot methods (Tables S2 and S3). Additionally, the enhanced detection sensitivity of this photo-initiated CRISPR one-pot reaction has also been validated using a visual lateral flow assay, demonstrating a clear advantage over the conventional CRISPR one-pot reaction system (Figure S14). Notably, our POIROTv2 retained robust detection sensitivity whether the RPA reaction time was set to 20 min, shortened to 10 min, or extended to 30 min; the only difference observed was a lower fluorescence signal at the shorter amplification time (Figure S15). Finally, to assess the analytical specificity of POIROTv2, we included human papillomavirus (HPV-16 and HPV-18) and influenza A virus (IAV) nucleic acids as extra targets and detected them in parallel with EBV and HCMV. Virus-specific sRNAs were designed for each target and tested under standard POIROTv2 conditions. The results showed that significant fluorescence signals were detected only in the presence of their corresponding targets, with no cross-reactivity observed between any sRNA and non-target sequences, highlighting its outstanding detection specificity (Figure S16).

HCMV- and EBV-Suspected Clinical Sample Detection by POIROTv2

After thoroughly evaluating the analytical performance of POIROTv2 on viral plasmid DNA, we further assessed its diagnostic utility and accessibility using HCMV and EBV clinical samples. Bronchoalveolar lavage fluid samples were collected from patients suspected of HCMV (n = 39) and EBV (n = 39) infection. Nucleic acids were extracted from all samples using a standardized extraction system (Figure 4a). These clinical samples were first analyzed using the gold-standard qPCR method (Figures S17−S20), using a cycle threshold (C_t) value of 40 as the cutoff for positive detection (Tables S4 and S5). As shown in Figure 4b,c, POIROTv2 exhibited perfect concordance with qPCR for HCMV sample detection, accurately identifying all 7 positive and 32 negative samples (Figure S21). Receiver operating characteristic (ROC) analysis yielded an area under the curve (AUC) of 1.00 (Figure 4d), reflecting an ideal diagnostic performance with 100% sensitivity and 100% specificity (Figure 4e). For the EBV-suspected clinical samples, POIROTv2 also demonstrated strong agreement with qPCR results, with one exception: one sample, which was qPCR-positive with a high C_t value (37.52), indicative of an extremely low viral load, was not detected by POIROTv2 (Figures 4f,g and S22). Despite this discrepancy, ROC analysis still yielded a high AUC value of 0.9568 (Figure 4h). Relative to the qPCR benchmark, POIROTv2 achieved a sensitivity of 93.75% and a specificity of 100% (Figure 4i), underscoring its high reliability and robust clinical applicability. Overall, these results indicate that POIROTv2 is a highly accurate and practical diagnostic platform for the detection of HCMV and EBV in clinical settings. Its performance closely aligns with that of the gold-standard qPCR method, supporting its potential as a rapid and user-friendly alternative for viral infection diagnosis.

CONCLUSIONS

Integrating nucleic acid isothermal amplification with the CRISPR system in a one-pot format offers a promising approach to enhance detection sensitivity. However, in such integrated systems, the CRISPR system, once activated by amplicons, can not only specifically cleave amplification templates but also nonspecifically degrade amplification primers. This dual activity severely compromises the amplification efficiency and limits the advantages of their combined use. To overcome these limitations, our research team previously developed a light-control strategy based on acylation of the 2′-OH group of crRNAs. By combining this approach with RPA reaction, we realized a photo-initiated CRISPR-based one-pot nucleic acid detection platform named POIROT. Since the acylation modification is independent of the nucleic acid sequence, this method markedly improved universality. However, each change in target sequence still necessitates reacylation of the corresponding crRNA—a step that, while straightforward, introduces a tangible bottleneck. This limitation prevents POIROT from fully escaping the shadow of sequence dependency, thus remaining a suboptimal solution.

In this study, we further optimized the POIROT platform to enhance its versatility. Capitalizing on the compatibility between split crRNA and the Cas12a protein, we specifically acylated the rRNA region to reversibly inhibit its binding to Cas12a, thereby temporarily suppressing CRISPR−Cas12a activity. After nucleic acid amplification is completed, UV light irradiation releases the PLGs from the rRNA, restoring CRISPR activity. This advancement led to the development of an upgraded one-pot detection system, POIROTv2. Compared to its predecessor, POIROTv2 maintains high sensitivity and specificity while achieving true “plug-and-play” universality—completely eliminating sequence-specific constraints. This significantly enhances both its applicability and its accessibility. When applied to clinical samples, POIROTv2 demonstrated excellent analytical performance comparable to the gold-standard qPCR method, indicating a strong potential for real-world diagnostics. Although the present work primarily focuses on the LbCas12a protein, the same strategy can be readily extended to other Cas12 orthologs, such as AsCas12a and ErCas12a, underscoring its broader adaptability. Moreover, although the current application emphasizes nucleic acid detection, this universal photo-control strategy holds promise for future expansion into broader biotechnological applications, such as gene editing, thereby offering new avenues for spatiotemporally precise regulation of CRISPR functions.

ASSOCIATED CONTENT

Supporting Information

The Supporting Information is available free of charge at https://pubs.acs.org/doi/10.1021/acs.analchem.5c05769.

^{1}H NMR spectrum of the 2-(2-nitrophenyl)propanol in $CDCl_3$; stability analysis of acylated rRNA after storage

https://doi.org/10.1021/acs.analchem.5c05769
Anal. Chem. XXXX, XXX, XXX−XXX

at room temperature and −20 °C for different durations; mass spectrum of original and cloaked rRNA; fluorescence kinetics of the photo-initiated CRISPR-Cas12a system under different UV light intensities; PAGE analysis of the effect of UV light irradiation on original rRNA; evaluation of the universality of photo-triggered CRISPR−Cas12a reactivation; component removal experiments to verify the POIROTv2 concept; sensitivity analysis of HCMV and EBV plasmid DNA by two-step assay; lateral flow assay after conventional CRISPR one-pot reaction and our photo-initiated one-pot reaction; evaluation of the effect of amplification time on the sensitivity of POIROTv2 assay; specificity analysis of the POIROTv2; qPCR assay for the detection of clinical HCMV and EBV samples; POIROTv2 assay for the detection of clinical HCMV and EBV samples; oligonucleotides sequences used in this study; performance comparison of POIROTv2 with other CRISPR one-pot detection methods; comparison of POIROTv2 with previous POIROT; C_t values obtained from the 39 clinical HCMV and EBV samples by qPCR assay (PDF)

AUTHOR INFORMATION

Corresponding Authors

Ling Jiang − *Key Laboratory of Chemical Biology & Traditional Chinese Medicine Research, Ministry of Education, Key Laboratory of Phytochemical R&D of Hunan Province, College of Chemistry and Chemical Engineering, Hunan Normal University, Changsha 410081, China*; Email: ljiang@hunnu.edu.cn

Erhu Xiong − *Key Laboratory of Chemical Biology & Traditional Chinese Medicine Research, Ministry of Education, Key Laboratory of Phytochemical R&D of Hunan Province, College of Chemistry and Chemical Engineering, Hunan Normal University, Changsha 410081, China*; orcid.org/0000-0002-9085-1858; Email: xiongeh@hunnu.edu.cn

Authors

Jinlian Du − *Key Laboratory of Chemical Biology & Traditional Chinese Medicine Research, Ministry of Education, Key Laboratory of Phytochemical R&D of Hunan Province, College of Chemistry and Chemical Engineering, Hunan Normal University, Changsha 410081, China*

Xingxiang Pu − *Department of Medical Oncology, Lung Cancer and Gastrointestinal Unit, Hunan Cancer Hospital & The Affiliated Cancer Hospital of Xiangya School of Medicine, Central South University, Changsha 410013, China*

Tongyan Yuan − *Key Laboratory of Chemical Biology & Traditional Chinese Medicine Research, Ministry of Education, Key Laboratory of Phytochemical R&D of Hunan Province, College of Chemistry and Chemical Engineering, Hunan Normal University, Changsha 410081, China*

Fang Peng − *Key Laboratory of Chemical Biology & Traditional Chinese Medicine Research, Ministry of Education, Key Laboratory of Phytochemical R&D of Hunan Province, College of Chemistry and Chemical Engineering, Hunan Normal University, Changsha 410081, China*

Jingjing Hu − *Key Laboratory of Chemical Biology & Traditional Chinese Medicine Research, Ministry of Education, Key Laboratory of Phytochemical R&D of Hunan Province, College of Chemistry and Chemical Engineering, Hunan Normal University, Changsha 410081, China*

Han Li − *Key Laboratory of Chemical Biology & Traditional Chinese Medicine Research, Ministry of Education, Key Laboratory of Phytochemical R&D of Hunan Province, College of Chemistry and Chemical Engineering, Hunan Normal University, Changsha 410081, China*

Bojie Chen − *Key Laboratory of Chemical Biology & Traditional Chinese Medicine Research, Ministry of Education, Key Laboratory of Phytochemical R&D of Hunan Province, College of Chemistry and Chemical Engineering, Hunan Normal University, Changsha 410081, China*

Jiaming Luo − *Key Laboratory of Chemical Biology & Traditional Chinese Medicine Research, Ministry of Education, Key Laboratory of Phytochemical R&D of Hunan Province, College of Chemistry and Chemical Engineering, Hunan Normal University, Changsha 410081, China*

Sheng Li − *Key Laboratory of Chemical Biology & Traditional Chinese Medicine Research, Ministry of Education, Key Laboratory of Phytochemical R&D of Hunan Province, College of Chemistry and Chemical Engineering, Hunan Normal University, Changsha 410081, China*

Yuling Teng − *Key Laboratory of Chemical Biology & Traditional Chinese Medicine Research, Ministry of Education, Key Laboratory of Phytochemical R&D of Hunan Province, College of Chemistry and Chemical Engineering, Hunan Normal University, Changsha 410081, China*

Xinyue Zhu − *Key Laboratory of Chemical Biology & Traditional Chinese Medicine Research, Ministry of Education, Key Laboratory of Phytochemical R&D of Hunan Province, College of Chemistry and Chemical Engineering, Hunan Normal University, Changsha 410081, China*

Weiming Chen − *Key Laboratory of Chemical Biology & Traditional Chinese Medicine Research, Ministry of Education, Key Laboratory of Phytochemical R&D of Hunan Province, College of Chemistry and Chemical Engineering, Hunan Normal University, Changsha 410081, China*

Qingqing Xie − *Key Laboratory of Chemical Biology & Traditional Chinese Medicine Research, Ministry of Education, Key Laboratory of Phytochemical R&D of Hunan Province, College of Chemistry and Chemical Engineering, Hunan Normal University, Changsha 410081, China*

Ronghua Yang − *Key Laboratory of Chemical Biology & Traditional Chinese Medicine Research, Ministry of Education, Key Laboratory of Phytochemical R&D of Hunan Province, College of Chemistry and Chemical Engineering, Hunan Normal University, Changsha 410081, China*; orcid.org/0000-0001-7873-6892

Complete contact information is available at: https://pubs.acs.org/10.1021/acs.analchem.5c05769

Author Contributions

#J.D. and X.P. contributed equally to this work.

Notes

The authors declare no competing financial interest.

ACKNOWLEDGMENTS

This work was supported by the National Natural Science Foundation of China (22274046, 22574049, 22504034, and 22334005), the Hunan Provincial Natural Science Foundation of China (2025JJ20018), the Outstanding Youth Foundation

of Hunan Provincial Education Department (24B0078), the Hunan Provincial Innovation Foundation for Postgraduate (CX20240533), and the Hunan Province College Students Research Learning and Innovative Experiment Project (2025105422618).

REFERENCES

(1) Guo, L.; Sun, X. H.; Wang, X. G.; Liang, C.; Jiang, H. P.; Gao, Q. Q.; Dai, M. Y.; Qu, B.; Fang, S.; Mao, Y. H.; Chen, Y. C.; Feng, G. H.; Gu, Q.; Wang, R. R.; Zhou, Q.; Li, W. SARS-CoV-2 detection with CRISPR diagnostics. *Cell Discov.* **2020**, *6*, 34.

(2) Larremore, D. B.; Wilder, B.; Lester, E.; Shehata, S.; Burke, J. M.; Hay, J. A.; Tambe, M.; Mina, M. J.; Parker, R. Test sensitivity is secondary to frequency and turnaround time for COVID-19 screening. *Sci. Adv.* **2021**, *7*, No. eabd5393.

(3) McDermott, A. Researchers race to develop in-home testing for COVID-19, a potential game changer. *Proc. Natl. Acad. Sci. USA* **2020**, *117*, 25956−25959.

(4) Loman, N. J.; Pallen, M. J. Twenty years of bacterial genome sequencing. *Nat. Rev. Microbiol.* **2015**, *13*, 787−794.

(5) Gavrilov, M.; Yang, J. Y.; Zou, R. S.; Ma, W.; Lee, C. Y.; Mohapatra, S.; Kang, J.; Liao, T. W.; Myong, S.; Ha, T. Engineered helicase replaces thermocycler in DNA amplification while retaining desired PCR characteristics. *Nat. Commun.* **2022**, *13*, 6312.

(6) Li, H. M.; Xie, Y.; Chen, F. M.; Bai, H. W.; Xiu, L. S.; Zhou, X. N.; Guo, X. K.; Hu, Q. Q.; Yin, K. Amplification-free CRISPR/Cas detection technology: challenges, strategies, and perspectives. *Chem. Soc. Rev.* **2023**, *52*, 361−382.

(7) Yu, C. X.; Lu, B. Y.; Tang, Y. D.; Zhuang, W. L.; Zhao, X.; Guo, L. L.; Meng, F. Z.; Li, B. L. A dual-position nucleic acid coding strategy for one-pot recognition of a pathogen and multiple drug-resistant mutations. *Chem. Eng. J.* **2025**, *512*, No. 162464.

(8) Liu, P. F.; Zeng, J. Y.; Jiang, C. C.; Du, J. L.; Jiang, L.; Li, S.; Zeng, F. X.; Xiong, E. H. Poly(vinylpyrrolidone)-Enhanced CRISPR-Cas System for Robust Nucleic Acid Diagnostics. *Anal. Chem.* **2024**, *96*, 15797−15807.

(9) De Felice, M.; De Falco, M.; Zappi, D.; Antonacci, A.; Scognamiglio, V. Isothermal amplification-assisted diagnostics for COVID-19. *Biosens. Bioelectron.* **2022**, *205*, No. 114101.

(10) Yang, H.; Chen, J. B.; Yang, S.; Zhang, T.; Xia, X. H.; Zhang, K. X.; Deng, S.; He, G. P.; Gao, H.; He, Q.; Deng, R. J. CRISPR/Cas14a-Based Isothermal Amplification for Profiling Plant MicroRNAs. *Anal. Chem.* **2021**, *93*, 12602−12608.

(11) Rolando, J. C.; Jue, E.; Barlow, J. T.; Ismagilov, R. F. Real-time kinetics and high-resolution melt curves in single-molecule digital LAMP to differentiate and study specific and non-specific amplification. *Nucleic Acids Res.* **2020**, *48*, No. e42.

(12) Barrangou, R.; Fremaux, C.; Deveau, H.; Richards, M.; Boyaval, P.; Moineau, S.; Romero, D. A.; Horvath, P. CRISPR provides acquired resistance against viruses in prokaryotes. *Science* **2007**, *315*, 1709−1712.

(13) Abudayyeh, O. O.; Gootenberg, J. S. CRISPR diagnostics. *Science* **2021**, *372*, 914−915.

(14) Chertow, D. S. Next-generation diagnostics with CRISPR. *Science* **2018**, *360*, 381−382.

(15) Pickar-Oliver, A.; Gersbach, C. A. The next generation of CRISPR-Cas technologies and applications. *Nat. Rev. Mol. Cell Biol.* **2019**, *20*, 490−507.

(16) Pacesa, M.; Pelea, O.; Jinek, M. Past, present, and future of CRISPR genome editing technologies. *Cell* **2024**, *187*, 1076−1100.

(17) Wang, Z. Y.; Liu, Y.; Zhou, F. L.; Wang, Y. F.; Zhou, X. The application of CRISPR-Cas in disease diagnosis and treatment. *Sci. China Chem.* **2023**, *66*, 2734−2742.

(18) Cao, L. X.; Wang, Z. Y.; Lei, C. Y.; Nie, Z. Engineered CRISPR/Cas Ribonucleoproteins for Enhanced Biosensing and Bioimaging. *Anal. Chem.* **2025**, *97*, 5866−5879.

(19) Yang, H.; Zhang, Y.; Teng, X. C.; Hou, H. W.; Deng, R. J.; Li, J. H. CRISPR-based nucleic acid diagnostics for pathogens. *TrAC Trends Anal. Chem.* **2023**, *160*, No. 116980.

(20) Liang, Y.; Zhang, J. G.; Xu, C. L.; Wang, J. J.; Han, W. S.; Yang, J. L.; Wu, S. X.; An, J. Y.; Liu, J. J.; Zhang, Z. Z.; Shi, J. J.; Zhang, K. X. Biomimetic Mineralized CRISPR/Cas RNA Nanoparticles for Efficient Tumor-Specific Multiplex Gene Editing. *ACS Nano* **2023**, *17*, 15025−15043.

(21) Shebanova, R.; Nikitchina, N.; Shebanov, N.; Mekler, V.; Kuznedelov, K.; Ulashchik, E.; Vasilev, R.; Sharko, O.; Shmanai, V.; Tarassov, I. Efficient target cleavage by Type V Cas12a effectors programmed with split CRISPR RNA. *Nucleic Acids Res.* **2022**, *50*, 1162−1173.

(22) Ding, X. M.; Lei, X. Y.; Yu, S. C. Efficient target cleavage by Type V Cas12a effectors programmed with split CRISPR RNA. *Biotechnol. Adv.* **2025**, *83*, No. 108629.

(23) Zeng, J. Y.; Liu, P. F.; Du, J. L.; Li, S.; Xiong, E. H.; Yang, R. H. Split crRNA-motivated amplification-free RNA testing with CRISPR-Cas12a. *Sci. China Chem.* **2025**, *68*, 789−801.

(24) Wen, M.; Zhou, M.; Huang, Z. X.; Wang, Y.; Wang, M. H.; Ding, Y.; Huang, X. Y.; Wang, B.; Wen, J. L.; Chen, T.; Zhang, P.; Chen, M.; Yang, C. Y.; Zhang, X. B.; Ke, G. L. Harnessing crRNA Transformer for Facile and Specific Nucleic Acid Detection. *Anal. Chem.* **2025**, *97*, 3964−3971.

(25) Xia, X. Y.; Liang, Z. G.; Xu, G. H.; Wei, F. D.; Yang, J.; Zhu, X. L.; Zhou, C. L.; Ye, J.; Hu, Q.; Zhao, Z.; Tang, B. Z.; Cen, Y. Split crRNA Precisely Assisted Cas12a Expansion Strategy for Simultaneous, Discriminative, and Low-Threshold Determination of Two miRNAs Associated with Multiple Sclerosis. *Anal. Chem.* **2025**, *97*, 2873−2882.

(26) Chen, Y. C.; Wang, X. P.; Zhang, J. Q.; Jiang, Q. Y.; Qiao, B.; He, B. X.; Yin, W. H.; Qiao, J.; Liu, Y. Split crRNA with CRISPR-Cas12a enabling highly sensitive and multiplexed detection of RNA and DNA. *Nat. Commun.* **2024**, *15*, 8342.

(27) Moon, J.; Liu, C. C. Asymmetric CRISPR enabling cascade signal amplification for nucleic acid detection by competitive crRNA. *Nat. Commun.* **2023**, *14*, 7504.

(28) Wang, J. Q.; Ye, X. F.; Liu, Y. F.; Li, W. T.; Zhang, X.; Zhang, W.; Yi, C. Q.; Liu, C. X. Regulating cleavage activity and enabling microRNA detection with split sgRNA in Cas12b. *Nat. Commun.* **2025**, *16*, 6392.

(29) Li, S. Y.; Cheng, Q. X.; Liu, J. K.; Nie, X. Q.; Zhao, G. P.; Wang, J. CRISPR-Cas12a has both and cleavage activities on single-stranded DNA. *Cell Res.* **2018**, *28*, 491−493.

(30) Dai, Y. F.; Wu, Y. F.; Liu, G. Z.; Gooding, J. J. CRISPR Mediated Biosensing Toward Understanding Cellular Biology and Point-of-Care Diagnosis. *Angew. Chem., Int. Ed.* **2020**, *59*, 20754−20766.

(31) Yuan, A. J.; Sha, R.; Xie, W. J.; Qu, G. B.; Zhang, H. Q.; Wang, H. L.; Le, X. C.; Jiang, G. B.; Peng, H. Y. RNA-Activated CRISPR/Cas12a Nanorobots Operating in Living Cells. *J. Am. Chem. Soc.* **2024**, *146*, 26657−26666.

(32) Chen, J. S.; Ma, E.; Harrington, L. B.; Da Costa, M.; Tian, X.; Palefsky, J. M.; Doudna, J. A. CRISPR-Cas12a target binding unleashes indiscriminate single-stranded DNase activity. *Science* **2018**, *360*, 436−439.

(33) Tang, Y. A.; Song, T. R.; Gao, L.; Yin, S. F.; Ma, M.; Tan, Y.; Wu, L. J.; Yang, Y.; Wang, Y. Q.; Lin, T.; Li, F. CRISPR-based ultrasensitive assay detects attomolar concentrations of SARS-CoV-2 antibodies in clinical samples. *Nat. Commun.* **2022**, *13*, 4667.

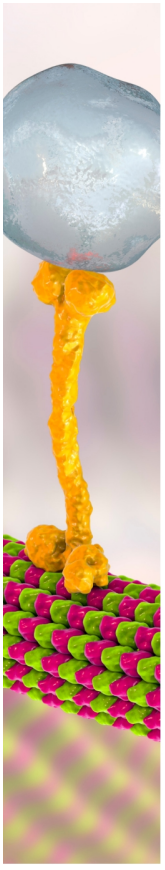
(34) Gootenberg, J. S.; Abudayyeh, O. O.; Lee, J. W.; Essletzbichler, P.; Dy, A. J.; Joung, J.; Verdine, V.; Donghia, N.; Daringer, N. M.; Freije, C. A. Nucleic acid detection with CRISPR-Cas13a/C2c2. *Science* **2017**, *356*, 438−442.

(35) Li, S. Y.; Cheng, Q. X.; Wang, J. M.; Li, X. Y.; Zhang, Z. L.; Gao, S.; Cao, R. B.; Zhao, G. P.; Wang, J. CRISPR-Cas12a-assisted nucleic acid detection. *Cell Discov.* **2018**, *4*, 20.

(36) Ding, X.; Yin, K.; Li, Z. Y.; Lalla, R. V.; Ballesteros, E.; Sfeir, M. M.; Liu, C. C. Ultrasensitive and visual detection of SARS-CoV-2

https://doi.org/10.1021/acs.analchem.5c05769
Anal. Chem. XXXX, XXX, XXX−XXX

using all-in-one dual CRISPR-Cas12a assay. *Nat. Commun.* **2020**, *11*, 4711.
(37) Lu, S. H.; Tong, X. H.; Han, Y.; Zhang, K.; Zhang, Y. Z.; Chen, Q. B.; Duan, J. Y.; Lei, X. L.; Huang, M. H.; Qiu, Y.; Zhang, D.-Y.; Zhou, X.; Zhang, Y.; Yin, H. Fast and sensitive detection of SARS-CoV-2 RNA using suboptimal protospacer adjacent motifs for Cas12a. *Nat. Biomed. Eng.* **2022**, *6*, 286−297.
(38) Yan, H.; Wen, Y. J.; Tian, Z. M.; Hart, N.; Han, S.; Hughes, S. J.; Zeng, Y. A one-pot isothermal Cas12-based assay for the sensitive detection of microRNAs. *Nat. Biomed. Eng.* **2023**, *7*, 1583−1601.
(39) Shao, F. C.; Park, J. S.; Zhao, G. J.; Hsieh, K. W.; Wang, T. H. Elucidating the Role of CRISPR/Cas in Single-Step Isothermal Nucleic Acid Amplification Testing Assays. *Anal. Chem.* **2023**, *95*, 3873−3882.
(40) Joung, J.; Ladha, A.; Saito, M.; Kim, N.-G.; Woolley, A. E.; Segel, M.; Barretto, R. P.; Ranu, A.; Macrae, R. K.; Faure, G. Detection of SARS-CoV-2 with SHERLOCK one-pot testing. *N. Engl. J. Med.* **2020**, *383*, 1492−1494.
(41) Arizti-Sanz, J.; Freije, C. A.; Stanton, A. C.; Petros, B. A.; Boehm, C. K.; Siddiqui, S.; Shaw, B. M.; Adams, G.; Kosoko-Thoroddsen, T.-S. F.; Kemball, M. E. Streamlined inactivation, amplification, and Cas13-based detection of SARS-CoV-2. *Nat. Commun.* **2020**, *11*, 5921.
(42) Chen, Y.; Mei, Y. X.; Zhao, X. H.; Jiang, X. Y. Reagents-Loaded, Automated Assay that Integrates Recombinase-Aided Amplification and Cas12a Nucleic Acid Detection for a Point-of-Care Test. *Anal. Chem.* **2020**, *92*, 14846−14852.
(43) Xia, S. M.; Chen, X. Single-copy sensitive, field-deployable, and simultaneous dual-gene detection of SARS-CoV-2 RNA via modified RT-RPA. *Cell Discov.* **2020**, *6*, 37.
(44) Wang, B.; Wang, R.; Wang, D. Q.; Wu, J.; Li, J. X.; Wang, J.; Liu, H. H.; Wang, Y. M. Cas12aVDet: A CRISPR/Cas12a-Based Platform for Rapid and Visual Nucleic Acid Detection. *Anal. Chem.* **2019**, *91*, 12156−12161.
(45) Zhao, T. T.; Yu, L.; Yin, M.; Huang, S. S.; Tian, R.; Zhong, C. Y.; Nan, F.; Zhang, H. F.; Tian, X.; Hu, Z. Enhanced One-Pot Cas12a-Based Nucleic Acid Detection via Epitope Insertion and Recruitment of Rad51. *Small* **2025**, *21*, No. e02417.
(46) Du, J. L.; Hu, J. J.; An, J.; Li, H.; Chen, B. J.; Luo, J. M.; Li, S.; Teng, Y. L.; Yuan, T. Y.; Zhu, X. Y.; Jiang, L.; Xiong, E. H.; Yang, R. H. Guanine-Quadruplex-Engineered crRNA Enables Light-Activated CRISPR/Cas12a System for Robust One-Pot Viral Assay. *Anal. Chem.* **2025**, *97*, 26580−26589.
(47) Hu, M. L.; Zhang, B. N.; Shan, Y. Y.; Cao, F.; Wang, Y. H.; Qi, W. W.; Wang, X.; Shen, Y. T.; Guo, X. Y.; Zhang, M. M.; Tian, T.; Xie, W.; Zhang, M. F.; Liang, F.; Pei, D. Q.; Zhou, X. M. Scalable modulation of CRISPR-Cas enzyme activity using photocleavable phosphorothioate DNA. *Nat. Commun.* **2025**, *16*, 5939.
(48) Chen, Y.; Xu, X. L.; Wang, J. C.; Zhang, Y. B.; Zeng, W. T.; Liu, Y. Z.; Zhang, X. J. Photoactivatable CRISPR/Cas12a Strategy for One-Pot DETECTR Molecular Diagnosis. *Anal. Chem.* **2022**, *94*, 9724−9731.
(49) Hu, M. L.; Qiu, Z. Q.; Bi, Z. R.; Tian, T.; Jiang, Y. Z.; Zhou, X. M. Photocontrolled crRNA activation enables robust CRISPR-Cas12a diagnostics. *Proc. Natl. Acad. Sci. U.S.A.* **2022**, *119*, No. e2202034119.
(50) Hu, M. L.; Liu, R. H.; Qiu, Z. Q.; Cao, F.; Tian, T.; Lu, Y. X.; Jiang, Y. Z.; Zhou, X. M. Light-Start CRISPR-Cas12a Reaction with Caged crRNA Enables Rapid and Sensitive Nucleic Acid Detection. *Angew. Chem., Int. Ed.* **2023**, *62*, No. e202300663.
(51) Tian, T.; Xiao, H. R.; Guo, X. Y.; Chen, Y. X.; Qiu, Z. Q.; Zhang, T.; Chen, M. Y.; Qi, W. W.; Cai, P. G.; Cheng, M.; Zhou, X. M. Identification of a key nucleotide influencing Cas12a crRNA activity for universal photo-controlled CRISPR diagnostics. *Nat. Commun.* **2025**, *16*, 6694.
(52) Zhou, W. Y.; Brown, W.; Bardhan, A.; Delaney, M.; Ilk, A. S.; Rauen, R. R.; Kahn, S. I.; Tsang, M.; Deiters, A. Spatiotemporal Control of CRISPR/Cas9 Function in Cells and Zebrafish using Light-Activated Guide RNA. *Angew. Chem., Int. Ed.* **2020**, *59*, 8998−9003.
(53) Liu, R.; Jiang, D. F.; Yun, Y. F.; Feng, Z.; Zheng, F. F.; Xiang, Y.; Fan, H. H.; Zhang, J. J. Photoactivatable Engineering of CRISPR/Cas9-Inducible DNAzyme Probe for Imaging of Nuclear Zinc Ions. *Angew. Chem., Int. Ed.* **2024**, *63*, No. e202315536.
(54) Chen, L.; Hu, M. L.; Zhou, X. M. Trends in developing one-pot CRISPR diagnostics strategies. *Trends Biotechnol.* **2025**, *43*, 98−110.
(55) Liu, P. F.; Lin, Y. T.; Zhuo, X. H.; Zeng, J. Y.; Chen, B. L.; Zou, Z.; Liu, G. H.; Xiong, E. H.; Yang, R. H. Universal crRNA Acylation Strategy for Robust Photo-Initiated One-Pot CRISPR-Cas12a Nucleic Acid Diagnostics. *Angew. Chem., Int. Ed.* **2024**, *63*, No. e202401486.
(56) Kadina, A.; Kietrys, A. M.; Kool, E. T. RNA cloaking by reversible acylation. *Angew. Chem., Int. Ed.* **2018**, *57*, 3059−3063.
(57) Habibian, M.; McKinlay, C.; Blake, T. R.; Kietrys, A. M.; Waymouth, R. M.; Wender, P. A.; Kool, E. T. Reversible RNA acylation for control of CRISPR-Cas9 gene editing. *Chem. Sci.* **2020**, *11*, 1011−1016.


CAS BIOFINDER DISCOVERY PLATFORM™
BRIDGE BIOLOGY AND CHEMISTRY FOR FASTER ANSWERS
Analyze target relationships, compound effects, and disease pathways
Explore the platform
CAS
A division of the American Chemical Society

https://doi.org/10.1021/acs.analchem.5c05769
Anal. Chem. XXXX, XXX, XXX−XXX